Materials Science-Poland, *Vol. 28*, *No. 1*, *2010*

Nitrogen doped carbon nanotubes and curved lamellas produced via pyrolysis of melamine by direct current arc discharge

R.I. ZHAO[1, 2], Y. MA[1], J. ZHANG[1*], F. LI[1], W. LIU[1], Q. CUI[1]

[1]National Laboratory of Superhard Materials, Jilin University, Changchun 130012, China

[2]Computer College, Jilin Normal University, Siping 136000, China

Nitrogen doped carbon nanostructures, including nanotubes and barrel like curved lamellas, were fabricated via the pyrolysis of a solo precursor, melamine, in a direct current arc discharge. The samples were characterized by elemental analysis, using XRD, XPS, TEM and SEM in parallel. The nitrogen concentration, determined from the elemental analysis, was shown to be lower than 5%. Nitrogen-based functional groups such as pyridine like structures, the pyrrolic or pyridonic structures, N-amine like structures and substitutional nitrogen within the graphene layers, were observed to coexist in the turbostratic carbon matrix. XRD patterns showed characteristic features of turbostratic carbons. TEM analysis of morphologies showed that nanostructures such as tubes and conglomerations of barrel like curved lamellas were present. The formation of bundles of nanotubes was further confirmed by SEM studies. The inhomogeneity in the morphologies of the nanostructures was attributed to the differences in their growth mechanisms.

Keywords: *carbon nanotubes; pyrolytic carbon; arc discharge*

1. Introduction

The studies of doping of carbon materials with nitrogen atoms has shown that the nitrogen-doping can obviously enhance mechanical, conducting, field emission, energy storage and electron transport properties and the catalytic activity in oxidation reactions of carbon materials [1–3]. Carbon nanotubes doped with nitrogen should exhibit novel electronic, chemical and mechanical properties [4]. In fact, the N doped bulk graphite systems have been the subject of investigations for a long time, due to their enhanced oxidation resistance and the possibility to adjust the crystallinity and graphitization. Nowadays, thanks to advances in nanoengineering and nanotechnology, the study of doping carbon nanostructures has entered a boom phase because

*Corresponding author, e-mail: zhangjian_lxf@yahoo.com.cn

these materials have potential applications as field effect transistors, logic circuits [5], sensors [6], promising materials for gas storage and adsorption [7], and as filler materials for reinforced composites [8], etc. Thus considerable efforts have been made to study the fabrication and the growth mechanism of the related carbon nanostructures with nitrogen as the dopant.

Up to now, only small quantities of nitrogen ($\leq$ 15 at. %) have been incorporated into carbon networks [9–12], which implies that the formation of C–N bonds is somehow difficult. From a thermodynamic point of view, this is reasonable, since segregation into pure carbon phases and nitrogen gas is much enhanced due partly to the strong triple bond in the nitrogen molecule. However, multiform nanostructures and inaugurating prototypes of devices have been obtained through various techniques, such as chemical vapour deposition (CVD) [1, 13], solvothermal techniques [14], direct current arc discharge [15], etc.

It is desirable that nitrogenous organic compounds be used as precursors for the fabrication of nitrogen containing nanostructures. Melamine seems to be an appropriate precursor of such a kind. In this paper, we report a new method to synthesize nitrogen doped carbon nanostructures in which the pyrolysis of melamine in a direct current arc discharge is involved. In this method, the pyrolysis of melamine takes place in a fast heating process generated by the direct current arc with the nitrogen rich gases as the working media, and the final products are formed via a quenching process for which the rate of temperature decrease ranges between 10^3 and 10^5 $K \cdot s^{-1}$. It is shown that nanotubes and nanobarrel like curved lamellas and sponge like networks formed by the conglomeration of those nanolamellas can be grown directly by this method.

2. Experimental

A sketch map of the direct current arc discharge system we used is shown in Fig. 1. In a typical experimental run, fine powders of melamine (purity $\geq$ 99.9%) and magnesium (purity $\geq$ 99.9%) were mixed together in an agate mortar in an appropriate ratio and cold pressed into pellets. The deliberate addition of magnesium was to make the pellets conductive, so that a direct current arc might be started. Carbonaceous conductive materials such as carbon fibres or filaments were not used, so that the final carbon product was totally produced from melamine, taking into account that the weight loss of graphite electrodes was negligible. Then a pellet was loaded in the water cooled graphite crucible, acting as the anode. A graphite rod (6 mm in diameter and 25 cm in long) was employed as the cathode. The reaction chamber was first evacuated to less than 1 Pa and washed several times with nitrogen (N_2, 99.999%). Then working gases such as nitrogen or ammonia (NH_3, 99.95%) were introduced into the chamber until the inner pressure reached the target value of 10–30 kPa. After the direct current arc was ignited, the input current was maintained at 100 A during the whole process of synthesis. However, the arc voltage increased gradually from 35 V to 45 V until the reactants were exhausted and the arc was quenched. After being pas-

sivated in N_2 for 6 h, powders were collected from the water-cooled collecting wall, which is made of copper. The powders were washed with concentrated hydrochloric acid, distilled water and ethanol repeatedly to remove the remnant reactants and magnesium compounds. The final product, which was black and had a fleece like texture, was then gathered.

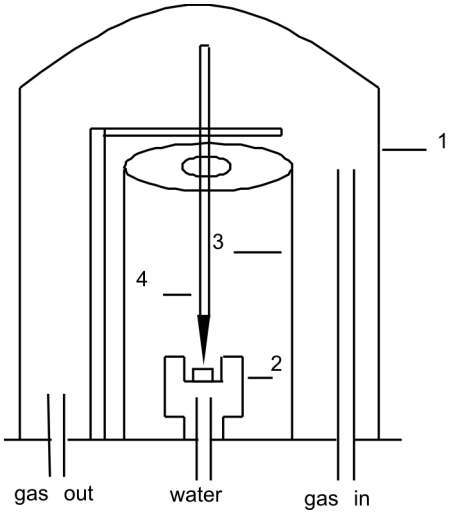

Fig. 1. A sketch diagram of the arc discharge system: 1 – reaction chamber, 2 – graphite crucible, 3 – copper collecting wall, 4 – graphite cathode. The crucible and the collecting wall are both cooled with water

The characterizations of the samples were carried out via elemental analysis, X-ray photoelectron spectroscopy (XPS), X-ray diffraction (XRD), transmission electron microscopy (TEM) and scanning electron microscopy (SEM). The compositions of the samples were examined by elemental analysis on a CHNS-O analyzer (Flash EA 1112 Series) through the conventional combustion method. The bonding states of the elements were studied via XPS on an EASY ESCA spectrometer (VG ESCA LAB MKII). The XRD patterns were obtained via a Rigaku Dmax-rA diffractometer operating with a copper target (λ = 1.54056 Å). The morphologies of the samples were taken on a H8100 transmission electron microscope operating at 200 KV and a Shimadzu Superscan SSX-550 scanning electron microscope operating at 15.0 kV.

3. Results and discussion

The chemical compositions of the samples synthesized under typical experimental conditions estimated through the combustion method are listed in Table 1. It can be seen that the products contain primarily carbon (82.51–89.37 wt. %). The doping level of nitrogen is relatively low (1.39–4.66 wt. %). Considerable amounts of hydrogen

(0.88–2.15 wt. %) are also present. The presence of other components of the products may be due to surface oxidation and absorption, which may be promoted by incorporating nitrogen in the carbon network. In addition, the influence of incomplete combustion of carbon species may not be ruled out entirely.

Table 1. Chemical compositions of the samples synthesized at typical experimental conditions estimated through the combustion method

Sample No.	Experimental conditions		Chemical composition [wt. %]			
	Gas	Pressure [kPa]	C	N	H	Other
1	N_2	10	86.54	2.39	0.97	10.10
2	N_2	30	89.37	1.39	0.88	8.36
3	NH_3	10	82.51	4.66	2.15	10.68
4	NH_3	30	86.58	3.19	1.01	9.22

The systematic variation of the compositions in relation to the experimental conditions may be roughly summarized as follows: (a) the powders produced in ammonia have higher nitrogen concentrations than those produced in nitrogen gas at the same gas pressure; (b) higher working gas pressures tend to lower the nitrogen concentration incorporated into the products. Taking the surface oxidation and adsorption into account, the contaminating oxygen and hydrogen are unavoidable. This effect may be enhanced by the intrinsic mesoporosity of the products, as shown below.

In fact, the compositions, structures, morphologies and other characteristics of the samples did not vary much, despite being subject to various experimental conditions. Hereafter, the samples obtained in the procedure under N_2 pressure of 10 kPa will be taken as the representative ones in the following discussions.

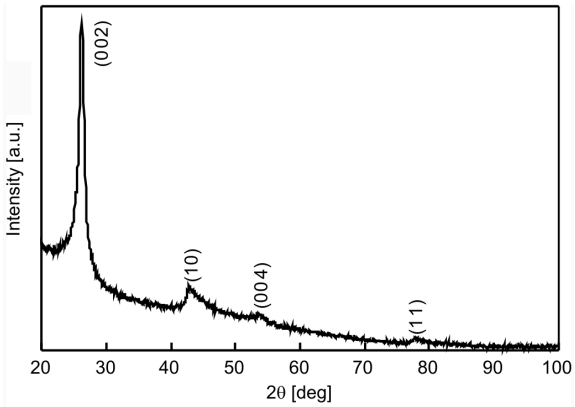

Fig. 2. A typical XRD pattern of the powders synthesized under the N_2 pressure of 10 kPa and I =100 A. The pattern is typical of all samples investigated in this study

The XRD pattern of the representative sample is shown in Fig. 2. A broadened peak at 26.22° and three weak diffraction bands at 42.91°, 53.48° and 78.03°, respec-

tively, are distinguished in the pattern. They can be indexed as typical (002), (10), (004) and (11) diffraction bands, respectively, for turbostratic carbons [16]. The (10) diffraction band shows a shape characteristic of a two-dimensionally ordered structure. The absence of (10l) bands or peaks indicates that there is no long range three-dimensional order of the graphite structure. The average thickness of the crystallized layers, L_c, can be roughly estimated to be about 10 nm through Scherrer's equation:

$$L_c = \frac{K\lambda}{B_{002}\cos\theta_{002}}$$

where θ_{002} is the diffraction angle and B_{002} is the full width at half maximum (FWHM) of (002) diffraction.

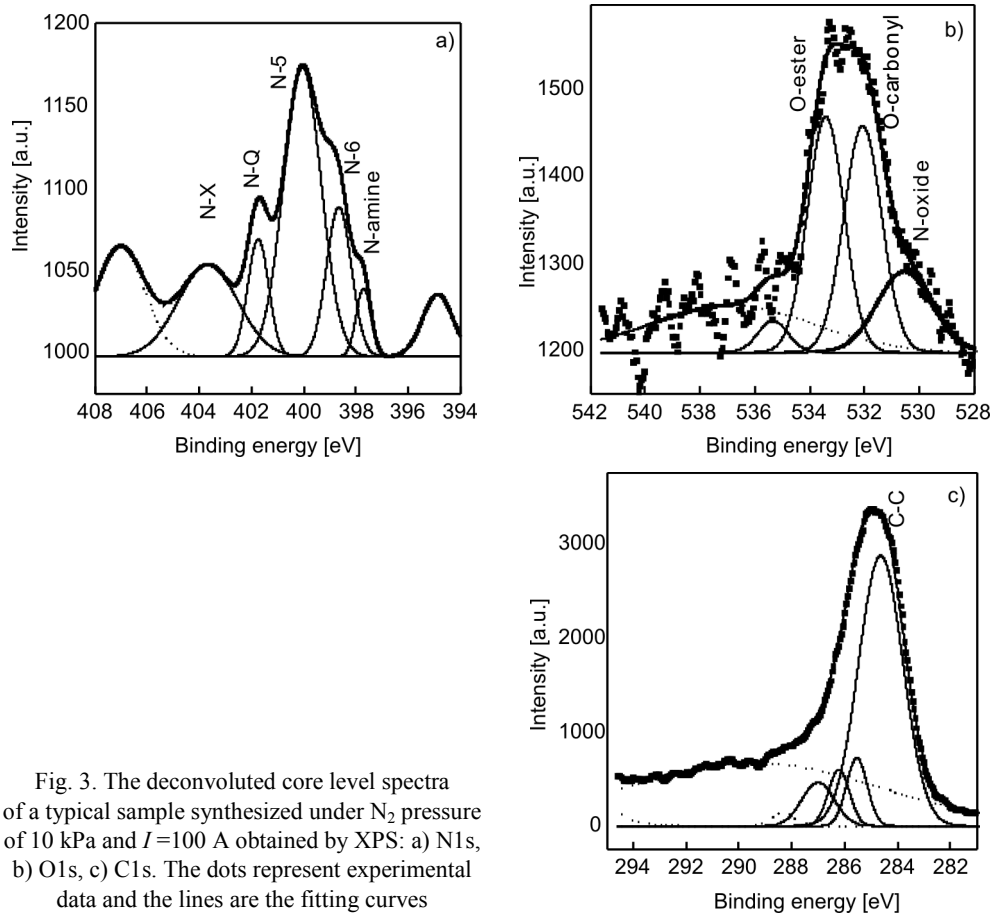

Fig. 3. The deconvoluted core level spectra of a typical sample synthesized under N_2 pressure of 10 kPa and I =100 A obtained by XPS: a) N1s, b) O1s, c) C1s. The dots represent experimental data and the lines are the fitting curves

The binding energy (BE) dispersion of the emitted core level electrons observed by XPS can reveal the chemical environment of the atoms in materials. In the present

case, turbostratic carbons are formed from radical atoms or small clusters in the arc discharge, thus one can assume that the experiments with other nitrogen containing carbons should be applied. Generally the results follow the observations with nitrogen-based functional groups of molecular organic compounds [17–19]. The N 1s core level spectra of our samples are fitted to Gaussian profiles, as shown in Fig. 3a. The component peaks are identified as nitride like species or aromatic N-amines with a BE of 397.7 eV, pyridinic nitrogen (N-6) with a BE of 398.7 eV, pyrrolic or pyridonic nitrogen (N-5) with a BE of 400.1 eV, substitutional nitrogen in the centre position in condensed polyaromatic systems, also called quaternary nitrogen (N-Q) with a BE of 401.7 eV, and nitrogen oxide or nitrate species (N-X) with a BE in the range of 402-405 eV. A schematic representation of the nitrogen based functional groups similar to those assigned in the present work may be found in the literature [19]. The O 1s core level spectra of our samples are also fitted to Gaussian profiles in a similar manner, as shown in Fig. 3b. Following the interpretation of XPS signals from oxygenated microporous carbons [20], the component peaks are identified as carbonyl oxygen atoms in esters, amides, anhydrides, and hydroxyls with a BE of 532.1 eV, ester oxygen atoms in esters and anhydrides with a BE of 533.4 eV, and nitrogen oxide or nitrate species (N-oxide) with a BE of 530.5 eV. These surface oxygen containing functional groups were most probably acquired during washing, since washing with acid solutions is a general way for modifying the surface chemistry of activated carbons to enable oxygen containing functional groups. Based on the above analyses, the deconvoluted C 1s core level spectra of the samples, as shown in Fig. 3c, can be readily explained. The major component with a BE of 284.6 eV is attributed to graphitic carbons (C–C). The minor component peaks are identified as carbons in C–N and/or C–O with a BE of 285.5 eV, carbons bonded to two N and/or O neighbours a BE of 286.3 eV, and carbons in C≡N and/or C=O with a BE of 287.1 eV, respectively.

The formation and mechanism of the bending and curling of graphene layers attracts considerable interest at present. In this study, nitrogen doped carbon nanostructures with exotic morphologies such as barrel like nanolamellas and bundles of nanotubes have been discovered. The so-called barrel like nanostructures are much shorter and less homogeneous with respect to their shapes and dimensions compared with ordinary nanotubes [16]. Typical TEM morphologies of the barrel like, or to be more precise in our case, bowl like curved lamellas, are shown in Fig. 4. It can be seen from Fig. 4a that the nanolamellas are curled and curved into irregular bowl like shapes. The characteristic calibre of these nanobowls is about 100 nm and the thickness is estimated to be about 10 nm. It is speculated that these curved lamellas may be the intermediate structures between the fully curled nanotubes and flat graphite planes. Structures with similar shapes but smaller sizes are also found (Fig. 4b). Presumably they are 10–20 nm in calibre and 2–5 nm thick. These curved lamellas conglomerated with one another, resulting in a sponge like structure with multitudinous mesopores and micropores. This structure may find potential usage in gas storage and catalyst support.

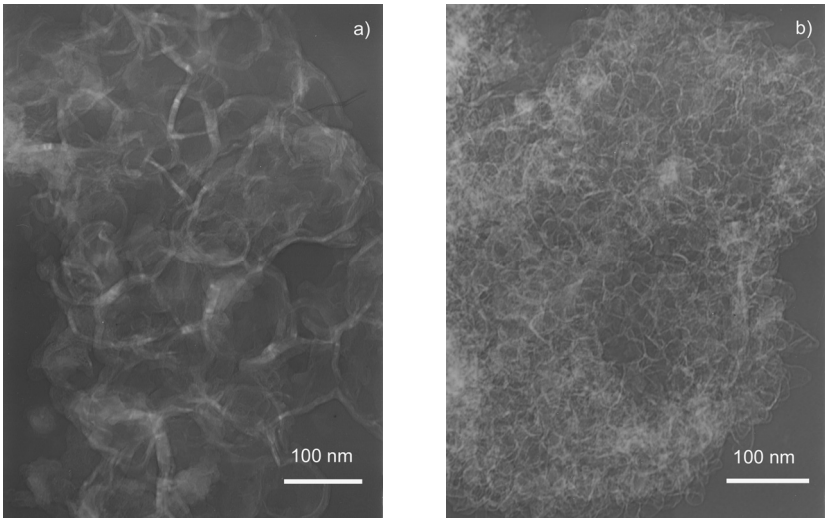

Fig. 4. TEM morphologies of N doped carbon nanomaterials with curved lamellar structures: a) the so-called barrel like nanolamellas with larger sizes, b) the sponge like conglomerations of smaller nanolamellas

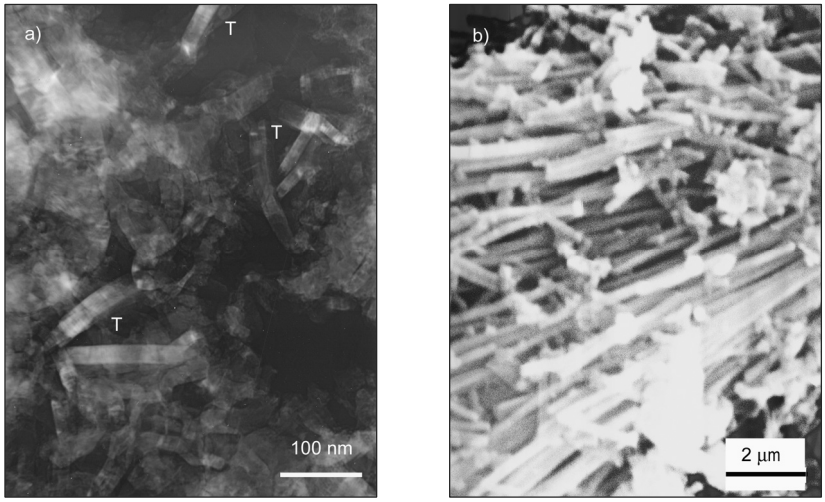

Fig. 5. The morphologies of nanotubes found in a representative sample synthesized under the N_2 pressure of 10 kPa and I =100 A: a) typical TEM morphology of several carbon nanotubes (marked as T) with their ends buried in amorphous clumps, b) typical SEM morphology of the nanotube bundles

Several nanotubes, 15–35 nm in diameter, are demonstrated in Fig. 5a (marked as T), with the coexistence of CN_x clumps. It is evident that the ends of the nanotubes are buried in those clumps. In Figure 5b, a typical SEM morphology of the nanotube bundles is demonstrated. The lengths of the nanotubes range from several micrometers to at least tens of micrometers. The nanotubes are somewhat crooked, indicating low

crystallinity. This is only reasonable, since the incorporation of nitrogen in the graphene network is anticipated to introduce large amounts of defects.

The growth of nanotubes and the clusters of nanolamellas seem to be mutually exclusive. In expansive regions, the nanotubes tend to coexist with only irregular-shaped particles (Fig. 5), absolutely non-concomitant with curved nanolamellas Meanwhile, the conglomerates seem to contain only species of barrel like nanolamellas. This phenomenon implies there is a difference between the growth mechanisms of the two kinds of nanostructures. As for the growth of carbon nanotubes, the so-called root-growth model has been proposed [1], in which vapours of the reactants dissolve in a molten catalyst to form eutectic particles and nanotubes then grow from these particles by supersaturation and segregation. From our TEM observations (Fig. 5), it can be seen that the ends of the nanotubes were embedded in surrounding clumps. Such a phenomenon implies that the root-growth model also provides a suitable explanation for the formation of N doped carbon nanotubes of our samples. Magnesium, melamine and the working gases such as nitrogen and ammonia react drastically with one another and nanosized particles of Mg_3N_2 and CN_x composites are formed. The vapours rich in carbon, nitrogen and CN radicals dissolve into these composite particles at the highly ionized central region of the arc plasma. The composite particles become supersaturated as they fly away from the high temperature arc region to the water-cooled collecting wall and the nucleation and segregation of the nanotubes take place.

As to the growth of the barrel like curved lamellas, a conceivable hypothesis is that they are formed with relatively low supersaturation of CN_x species, which results in low growth rates. They grow faster within the graphene planes than in the perpendicular direction and develop into lamellas with high aspect ratios. The lamellas are so thin that the rolling process could proceed easily via the combined effect of the extremely high temperature, the bombardment of radicals and the quenching process. However, the curling of the lamellas occurred in all direction simultaneously, due to the high defect density induced by the incorporation of N atoms. Thus, instead of seamless co-axial cylinders, irregular barrel like structures are formed.

It should be noted that no materials with the layered structure such as graphite were present in the starting materials. This implies that the direct formation of doped carbon nanostructures such as nanotubes, fullerenes, etc., using nitrogen-rich precursors via certain techniques such as arc discharge or laser ablation is possible. This may be a new and promising route for the synthesis of doped carbon nanostructures and further work has to be carried out for the optimization of the experiments.

4. Conclusion

Nanocrystalline carbon materials such as nanotubes, fullerenes and related structures are a high profile subject in science and technology, due to their potential usages in nanoengineering as well as their other attractive properties. The doping of these

materials opens up new routes to nanoscale electronics. Various techniques such as arc discharge laser ablation and CVD, etc. have been employed to produce those doped nanostructures. In this study, the preparation of N doped carbon nanostructures via the pyrolysis of a solo precursor, melamine, was demonstrated. The final product had been characterized by various techniques used in parallel. The doping level was shown to be lower than 5 wt. % by elemental analysis via the combustion method. XPS studies revealed that N atoms occupying the substitutional sites, the pyridine like sites, the pyrrolic or pyridonic sites and N-amine like sites coexisted in the carbon matrix. XRD patterns showed characteristic features of turbostratic carbons. In the TEM morphologies, nanostructures such as tubes and conglomerations of barrel like curved lamellas were found and attributed to different growth mechanisms. The formation of bundles of nanotubes was further confirmed by SEM studies.

Acknowledgements

This work was supported by the Natural Science Foundation of China (grant No. 50772043, 50372023, 50334030), the National Basic Research Program of China (grant No. 2001CB711201, 2005CB724400), the research startup foundation of Jilin University (No. 419080103460) and the Research Fund for the Doctoral Program of Higher Education of China (20070183175).

References

[1] TERRONES M., AJAYAN P.M., BANHART F., BLASE X., CARROLL D.L., CHARLIER J.C., CZERW R., FOLEY B., GROBERT N., KAMALAKALAN R., REDLICH PH., RŰHLE M., SEEGER T., TERRONES H., Appl. Phys. A, 74 (2002), 355.

[2] STÖHR B., BOEHM H., SCHLÖGL R., Carbon, 29 (1991), 707.

[3] BANDOSZ T., J. Colloid Interf. Sci., 246 (2002), 1.

[4] TERRONES M., JORIO A., ENDO M., RAO A.M., KIM Y.A., HAYASHI T., TERRONES H., CHARLIER J.C., DRESSELHAUS G., DRESSELHAUS M.S., Mater. Today, 7 (2004), 30.

[5] AVOURIS P., Chem. Phys., 281 (2002), 429.

[6] DOROZHKIN P.S., TOVSTONOG S.V., GOLBERG D., ZHAN J., ISHIKAWA Y., SHIOZAWA M., NAKANISHI H., NAKATA K., BANDO Y., Small, 1 (2005), 1088.

[7] YANG C.M., NOGUCHI H., MURATA K., YUDASAKA M., HASHIMOTO A., IIJIMA S., KANEKO K., Adv. Mater., 17 (2005), 866.

[8] THOSTENSON E.T., LI C., CHOU T.W., Compos. Sci. Technol., 65 (2005), 491.

[9] TERRONES M., REDLICH PH., GROBERT N., TRASOBARES S., HSU W.K., TERRONES H., ZHU Y.Q., HARE J.P., CHEETHAM A.K., RŰHLE M., KROTO H.W., WALTON D.R.M., Adv. Mater., 11 (1999), 655.

[10] TERRONES M., GROBERT N., OLIVARES J., ZHANG J.P., TERRONES H., KORDATOS K., HSU W.K., HARE J.P., TOWNSEND P.D., PRASSIDES K., CHEETHAM A.K., KROTO H.W., WALTON D.R.M., Nature, 388 (1997), 52.

[11] SEN R., SATISHKUMAR B.C., GOVINDARAJ S., HARIKUMAR K.R., RENGANATHAN M.K., RAO C.N.R., J. Mater. Chem., 7 (1997), 2335.

[12] SEN R., SATISHKUMAR B.C., GOVINDARAJ S., HARIKUMAR K.R., RAINA G., ZHANG J.P., CHETHAM A.K., RAO C.N.R., Chem. Phys. Lett., 287 (1998), 671.

[13] TERRONES M., TERRONES H., GROBERT N., HSU W.K., ZHU Y.Q., KROTO H.W., WALTON D.R.M., KOHLER-REDLICH PH., RŰHLE M., ZHANG J.P., CHEETHAM A.K., Appl. Phys. Lett., 75 (1999), 3932.

[14] WU C., GUO Q., YIN P., LI T., YANG Q., XIE Y., J. Phys. Chem. B, 109 (2005), 2597.

[15] GLERUP M., STEINMETZ J., SAMAILLE D., STÉPHAN O., ENOUZ S., LOISEAU A., ROTH S., BERNIER P., Chem. Phys. Lett., 387 (2004), 193.
[16] LEIS J., PERKSON A., ARULEPP M., KÄÄRIK M., SVENSSON G., Carbon, 39 (2001), 2043.
[17] STAŃCZYK K., DZIEMBAJ R., PIWOWARSKA Z., WITKOWSKI S., Carbon, 33 (1995), 1383.
[18] WEIDENTHALER C., LU A., SCHMIDT W., SCHÜTH F., Micropor. Mesopor. Mat., 88 (2006), 238.
[19] KAPTEIJN F., MOULIJN J., MATZNER S., BOEHM H., Carbon, 37 (1999), 1143.
[20] SU F., ZHAO X.S., LV L., ZHOU Z., Carbon, 42 (2004), 2821.

Received 27 April 2009
Revised 10 September 2009